

Learning Flexible Forward Trajectories for Masked Molecular Diffusion

Hyunjin Seo^{1,2*}, Taewon Kim^{1,2*}, Sihyun Yu¹, SungSoo Ahn^{1†}

Korea Advanced Institute of Science and Technology (KAIST)¹, Polymerize²
 {bella72, maxkim139, sihyun.yu, sungsoo.ahn}@kaist.ac.kr

Abstract

Masked diffusion models (MDMs) have achieved notable progress in modeling discrete data, while their potential in molecular generation remains underexplored. In this work, we explore their potential and introduce the surprising result that naïvely applying standards MDMs severely degrades the performance. We identify the critical cause of this issue as a *state-clashing problem*—where the forward diffusion of distinct molecules collapse into a common state, resulting in a mixture of reconstruction targets that cannot be learned using typical reverse diffusion process with unimodal predictions. To mitigate this, we propose **Masked Element-wise Learnable Diffusion (MELD)** that orchestrates per-element corruption trajectories to avoid collision between distinct molecular graphs. This is achieved through a parameterized noise scheduling network that assigns distinct corruption rates to individual graph elements, *i.e.*, atoms and bonds. Extensive experiments on diverse molecular benchmarks reveal that **MELD** markedly enhances overall generation quality compared to element-agnostic noise scheduling, increasing the chemical validity of vanilla MDMs on ZINC250K from 15% to 93%. Furthermore, it achieves state-of-the-art property alignment in conditional generation tasks.

1 Introduction

Molecular generation is crucial in a variety of real-world applications, such as drug discovery [62, 67] and material design [24, 71]. However, the task remains challenging due to the extremely large and complex nature of the chemical space [9, 30, 68]. With the remarkable recent progress in deep generative models [2, 32, 44, 53], many approaches have attempted to tackle this problem by training a neural network that learns molecular distributions from large molecular datasets, demonstrating a strong promise in accelerating molecule discovery [23, 25, 28, 37, 59, 66].

In particular, recent approaches have focused on exploring diffusion models [27, 28, 33, 35, 37, 66] that can learn a molecular distribution, inspired by their great success in other data domains [2, 15, 31, 41, 46, 56, 63]. These models learn to recover original molecules from corrupted versions through a denoising process, where the corruption typically involves altering types of atoms and bonds (*e.g.*, changing a carbon atom to nitrogen, or a single bond to a double bond).

Meanwhile, researchers have proposed masked diffusion models (MDMs) [2, 5, 55, 60], to make diffusion models specialized for modeling discrete data by defining a diffusion process more suitable in discrete space. Specifically, MDMs define corruption (*i.e.*, the forward process) as element masking and train the model (*i.e.*, the reverse process) to infill the masked element. Intriguingly, MDMs show great stability and scalability, demonstrating comparable or even better performance with previous state-of-the-art generative modeling schemes for discrete data, such as autoregressive language

*Equal Contribution.

†Corresponding Author.

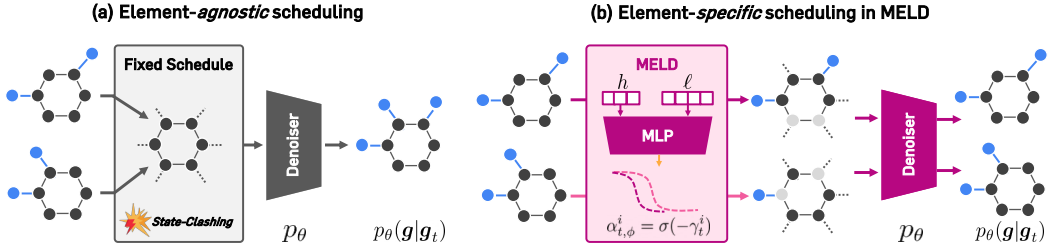


Figure 1: Comparison between (a) Element-agnostic noise scheduling and (b) Element-specific noise scheduling. The former results in an issue denoted as *state-clashing*, leading to generation of invalid molecules. **MELD** mitigates this with element-specific noise schedule, effectively orchestrating the forward process to minimize state-clashings.

models [17, 75] or high-resolution text-to-image generation [4]. Despite their success and great potential in other domains, applying MDMs to molecular graphs is still underexplored.

In this work, we focus on applying MDMs for molecular generation. Surprisingly, unlike other domains, a naïve adaptation of existing MDMs to molecular graphs results in significantly worse performance than other recent molecular generation methods, often generating chemically invalid structures. We argue that this phenomenon stems from *state-clashing problem*—molecular graphs with different properties and semantics easily collapse into a common intermediate state in the forward process (see Figure 1 (a) for an illustration). We trace this limitation to the design of the noise scheduling in existing MDMs, which assumes a fixed, uniform transition probability across all nodes and edges. However, MDMs learn the reverse process as unimodal predictions, which prevents them from capturing the highly multimodal distribution of the true posterior. This leads to generating samples that violate the chemical rules or significantly deviate from the target distribution.

To address this, we introduce **MELD** (Masked Element-wise Learnable Diffusion), a novel MDM for molecular graph generation. The main idea of our method is to alleviate the state-clashing problem by proposing an *element-wise learnable forward process*, which mitigates the state-clashing problem by generating trajectories in the way of minimizing the occurrence of state-clashing. To this end, we introduce a parameterized noise scheduling network to yield distinct corruption rates for individual graph elements (*i.e.*, for nodes or edges). During training, we jointly optimize the forward (*i.e.*, noise scheduling network) and the reverse process (*i.e.*, MDM denoiser network). Intuitively, by assigning per-element trajectories, **MELD** organizes the forward process such that the probability of molecules being collapsed to the same intermediate state (see Figure 1 (b)) is minimized. Through such evasion, **MELD** produces samples that are chemically sound and valid.

We extensively evaluate the effectiveness of **MELD** on diverse molecule benchmarks including QM9 [52], Polymers [64], and ZINC250K [19] datasets. First, we demonstrate that **MELD** gains substantial improvements in chemical validity and distributional similarity over standard MDMs. Furthermore, compared with other state-of-the-art molecular generation or optimization methods, **MELD** achieves comparable or superior performance in both unconditional and property-conditioned molecule generation tasks. For instance, on the conditional generation setup on the polymer dataset, **MELD** achieves up to a 16.5% enhancement in property alignment compared to the state-of-the-art diffusion model.

Our contributions are threefold:

- We identify a key limitation in applying standard masked diffusion models to molecular generation—the use of an element-agnostic noise schedule—which leads to frequent *state-clashing*.
- We present **MELD**, a novel masked diffusion framework that mitigates the state-clashing problem by learning per-element noise schedules, allowing adaptive corruption trajectories tailored to individual molecular components.
- **MELD** significantly improves the validity over unified noise scheduling baselines, demonstrating strong performance in both unconditional and property-conditioned molecule generation.
- We conduct extensive analysis, revealing that (1) in general, the denoiser module prefers unmasking graph elements in a *node-first* manner, empirically verified through case studies, and (2) higher diversity (*i.e.* variance) is observed in the later phases of the learned noise schedule, suggesting state-clashing to be intensified in later steps of noising, as hypothesized.

2 Related Work

Masked diffusion models (MDMs). MDMs have emerged as a powerful generative modeling scheme for discrete data generation. Initially, D3PM [2] introduces an absorbing mask token into the forward process and establishes a conceptual bridge between discrete diffusion and masked language modeling. Additionally, in image generation, MaskGIT [5] shows that generative modeling based on unmasking enables fast and qualitatively comparable high-fidelity image synthesis compared with left-to-right autoregressive decoding. More recent efforts have further refined MDMs to close the performance gap with autoregressive models (AR) [17, 65, 75]. Notably, MD4 and [60] and MDLM [55] show that the diffusion objective can be simplified as a weighted integral of cross-entropy terms and that the model can achieve state-of-the-art performances over previous diffusion models. Our work also focuses on MDMs, but we explore the applications of MDMs for molecules.

Diffusion models for molecules. The success of diffusion models for image [5, 15, 31, 41, 46, 54, 56, 63] and text generation [2, 3, 14, 36, 55, 60] has inspired researchers to explore their potential in molecule domain. A surge of studies [27, 28, 33, 37, 66, 70] have been proposed to generate de novo molecules, competing with sequential models [21, 22, 25, 57, 59] that iteratively constructs a graph by adding graph elements. These efforts can be broadly categorized into two approaches: (1) Score-based molecule diffusion approaches [27, 28, 35] adopt continuous noise on molecular graphs using stochastic differential equations (SDEs) [63]. During the reverse diffusion process, they train a score function to reverse this diffusion, relaxing discrete atoms/bonds into a continuous space. (2) Discrete diffusion-based approaches [18, 29, 37, 66] apply discrete noise through Markovian transitions to nodes and edges in molecular graphs. Then they train a denoising neural network to reconstruct perturbed atom and bond types.

Despite progress in the two aforementioned directions, masked diffusion frameworks remain under-explored for molecular generation. A preliminary application was explored in [33], but it generates atoms in an autoregressive manner, limiting its ability to exploit the parallelized reconstruction of MDMs. In contrast, we propose a new MDM for molecular graphs by focusing on the state-clashing problem occurring in the forward process, while preserving the parallelism inherent to MDMs.

3 MELD: Masked element-wise learnable diffusion

In this section, we introduce **MELD**, a masked diffusion model (MDM) for molecular graph generation that jointly learns per-graph-element corruption rate and the denoising model. As we will explain, our proposed design alleviates the state-clashing problem by producing easily distinguishable forward trajectories for each molecular component.

3.1 Main algorithm

Similar to standard diffusion models [15, 41, 46, 49], we characterize our masked molecular diffusion process using a forward and reverse process. The forward process progressively corrupts a clean molecular graph through a sequence of Markov transitions, while the reverse process starts from a sample from the prior distribution and iteratively reconstructs the original sample. Unlike the existing work on molecular diffusion models, our key difference is to (1) use masking/unmasking-based forward/reverse transitions (respectively), (2) introduce element-wise parameterization of the forward process, and (3) jointly learn the forward process in addition to the reverse process.

Problem definition. We consider the task of generating molecules represented as graphs, denoted by $\mathcal{G} = (\mathcal{V}, \mathcal{E})$, where \mathcal{V} is a set of N atoms (nodes) and \mathcal{E} a set of bonds (edges). We encode \mathcal{V} with a categorical feature $\mathbf{x} = (x^i)_{i=1}^N$, where each $x^i \in \{1, \dots, A\}$ indicates the atom type of node i among the A possible types with one category reserved for [mask] token. Similarly, we encode \mathcal{E} as a categorical feature $\mathbf{e} = (e^{ij})_{i,j=1}^N$ where each $e^{ij} \in \{1, \dots, B\}$ is the bond type between the atoms i and j , with two categories reserved for the “no bond” and [mask] tokens.

Since the graph is an abstract object, our implementations rely on explicit representation $\mathbf{g} = (\mathbf{x}, \mathbf{e})$ of graph \mathcal{G} . Finally, our goal is to train a graph generator from the data distribution $q(\mathbf{g})$. To this end, we introduce a forward process $q_\phi(\mathbf{g}_t | \mathbf{g}_{t-1})$ and a reverse process $p_\theta(\mathbf{g}_{t-1} | \mathbf{g}_t)$, parameterized by ϕ and θ , respectively.

Forward and reverse diffusion processes. At each timestep t , the forward diffusion process q_ϕ progressively corrupts atoms and bonds by stochastically transitioning them into a masked state, denoted by `[mask]`. This transition is governed by Markov kernels defined with a monotonically increasing sequence $\beta_t \in [0, 1]$. Specifically, the Markov kernels are defined as

$$q_\phi(x_t^i | x_{t-1}^i) = \begin{cases} \beta_{t,\phi}^i & \text{if } x_t^i = \text{[mask]} \\ 1 - \beta_{t,\phi}^i & \text{if } x_t^i = x_{t-1}^i \end{cases}, \quad q_\phi(e_t^{ij} | e_{t-1}^{ij}) = \begin{cases} \beta_{t,\phi}^{ij} & \text{if } e_t^{ij} = \text{[mask]} \\ 1 - \beta_{t,\phi}^{ij} & \text{if } e_t^{ij} = e_{t-1}^{ij} \end{cases}. \quad (1)$$

Note that prior works [27, 28, 35, 37, 66] have assumed the forward diffusion process as a *fixed* transition probability that is uniform across elements (vertices and edges). In contrast, our work introduces an additional degree of freedom, represented by the parameter ϕ , which allows flexible modeling of the forward diffusion process to overcome the state-clashing problem. Importantly, the kernels are distinct for each vertex, which means that the forward diffusion process is no longer equivariant, *i.e.*, the marginal distribution of an intermediate state is affected by permutation.

Next, the reverse process recovers the clean graph from a noisy state \mathbf{g}_t , and we learn this process through a model $p_\theta(\mathbf{g}_{t-1} | \mathbf{g}_t)$. In particular, each denoising step is formalized as the product over nodes and edges [66]:

$$p_\theta(\mathbf{g}_{t-1} | \mathbf{g}_t) = \prod_{v \in \mathcal{V}} p_\theta(x_{t-1}^i | \mathbf{g}_t) \prod_{e \in \mathcal{E}} p_\theta(e_{t-1}^{ij} | \mathbf{g}_t). \quad (2)$$

Training objective. In practice, the denoising network is trained to directly predict the original graph \mathbf{g}_0 from the noisy intermediate state \mathbf{g}_t , eliminating the need for recursive sampling [37, 66]. This is achieved by training the model based on a cross-entropy loss between the predicted logits and the ground-truth node and edge categories [55, 60]:

$$\mathcal{L}(\theta, \phi) := -\mathbb{E}_{t, \mathbf{g}, \mathbf{g}_t} \left[\sum_{1 \leq i \leq N} \frac{\dot{\alpha}_{t,\phi}^i}{1 - \alpha_{t,\phi}^i} \log p_\theta(x^i | \mathbf{g}_t) + \lambda \sum_{1 \leq i, j \leq N} \frac{\dot{\alpha}_{t,\phi}^{ij}}{1 - \alpha_{t,\phi}^{ij}} \log p_\theta(e^{ij} | \mathbf{g}_t) \right], \quad (3)$$

where the expectation is over $\mathbf{g} \sim q(\cdot)$, $\mathbf{g}_t \sim q_\phi(\cdot | \mathbf{g})$, $t \sim \text{Unif}[0, 1]$. Furthermore, we let $\alpha_{t,\phi}^i = \prod_{t'=t}^T \beta_{t',\phi}^i$ and $\dot{\alpha}_{t,\phi}^i$ is the derivative $\alpha_{t,\phi}^i$ with respect to t , and $\lambda > 0$ is a hyperparameter that balances the contributions of node- and edge-level reconstruction introduced in prior works [37, 66]. Note that naïvely applying gradient-based optimization to Monte Carlo estimation of the loss equation 3 does not incorporate the dependency on ϕ . We use straight-through gumbel softmax trick (STGS) trick [20] to address this issue, as explained further in Section 3.3.

3.2 Formalizing the state-clashing problem

Here, we describe the *state-clashing problem* which naturally arise for training MDMs on graphs without learning the forward process, *i.e.*, set $\beta_{t,\phi}^i$ to some constant β_t for all node i and similarly for the edges. In a nutshell, state-clashing refer to the phenomenon where semantically distinct molecules are corrupted into the same intermediate state, due to the nature of the constant forward process in MDMs. Consequently, the model trained with such constant forward process struggles to infer the correct reconstruction target, resulting in outputs that fail to preserve molecular validity or semantic coherence (see Figure 1 for an illustration). This is particularly pronounced in molecules with symmetric motifs, to which the number of immediate parent states grows by the number of permutations that leave the motif invariant.

Formally, note that the diffusion model loss in Equation 3 can be expressed as:

$$\mathbb{E}_t [\text{KL}(p(\mathbf{g} | \mathbf{g}_t), p_\theta(\mathbf{g} | \mathbf{g}_t))], \quad p(\mathbf{g} | \mathbf{g}_t) \propto p(\mathbf{g}_t | \mathbf{g}) p(\mathbf{g}). \quad (4)$$

The main problem is that $p(\mathbf{g} | \mathbf{g}_t)$ can be highly *multimodal*, *i.e.*, there exists many graph \mathbf{g} with non-zero probabilities of $p(\mathbf{g}_t | \mathbf{g})$. However, the parameterized diffusion model $p_\theta(\mathbf{g} | \mathbf{g}_t) = \prod_{1 \leq i \leq N} p(x^i | \mathbf{g}_t) \prod_{1 \leq i, j \leq N} p(e^{ij} | \mathbf{g}_t)$ is *unimodal*, as it predicts each node and edge independently, typically resulting in a single mode centered around an average graph. Furthermore, due to the mode-covering property of KL divergence, the reverse diffusion model trained with Equation 3 tends to converge to a high-entropy distribution—the model compensates for its inability to represent multiple modes by spreading its probability mass broadly around the single mode, as illustrated

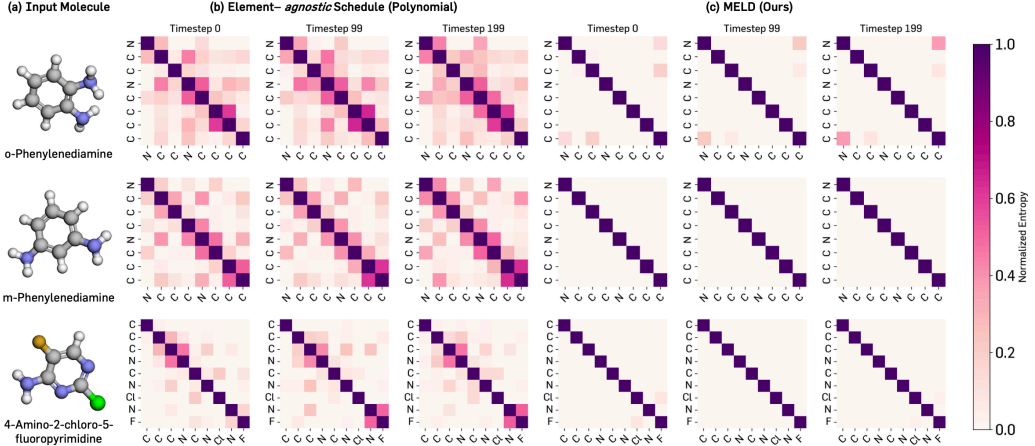


Figure 2: Visualization of prediction entropy for various molecule types. First and second row are prediction matrices generated with nitrogen bonds masked, while the third row depict generations with chlorine bonds masked. From left to right, (a) 3D renderings of the input molecules, (b) Masked-diffusion model predictions using fixed polynomial noise schedule, and (c) Predictions produced by **MELD**. Brighter colors indicate lower uncertainty (*i.e.*, higher confidence). Note that predictions are being made for all locations, regardless of their entropy values.

in the first and second rows of Figure 2.[†] In addition, we visualize the model’s predictions for 4-Amino-2-Chloro-5-Fluoropyrimidine when only the Chlorine bonds are masked (*i.e.*, hidden). Owing to the inherent asymmetry of the pyrimidine backbone, the state-clashing issue is less pertinent than Phenylendiamine isomers. As a result, we observe increased prediction confidence even in MDMs employing unified scheduling, underscoring the necessity of addressing the state-clashing.

We note that this issue is not unique to MDMs, but it does become significantly more severe for MDMs. This is because masking operations tend to absorb diverse input graphs into indistinguishable intermediate states, unlike substitution-based corruption in standard discrete diffusion models, which preserves more structural variation and retains partial identity throughout the trajectory.

3.3 Algorithm details

Learnable element-wise embedding. To alleviate the state-clashing through learning element-wise noise scheduling, one should provide rich graph information to scheduling network to ensure the forward diffusion trajectories among graph components to have as less probability of state-clashing as possible. One possible approach is to incorporate graph positional encodings [10, 40] as the conditioning input. However, such encodings often fail to differentiate symmetric structures such as those found in aromatic rings [34, 43].

Thus, we consider learnable element-wise embeddings over the graph elements that assigns distinct noise schedules even under symmetric motifs, and use it for an input to the noise scheduling network. Specifically, we assign a learnable embedding matrix $\mathbf{H} \in \mathbb{R}^{D \times N}$ and consider its i -th column \mathbf{h}^i as node-wise embedding of i -th node x^i , where $N > 0$ is a number of nodes and D is the embedding dimension. For an edge embedding of the edge connecting x^i and x^j , set $\mathbf{h}^{ij} = \mathbf{h}^i + \mathbf{h}^j$ as the corresponding embedding.

Time-dependent noise scheduling network. From each node embedding \mathbf{h}^i and edge embedding \mathbf{h}^{ij} , our noise embedding network f_ϕ computes the corresponding noise scheduling at each element. Specifically, we construct f_ϕ as follows:

$$f_\phi(\mathbf{h}, \ell) := \text{MLP}_\psi(\mathbf{W}_\ell \mathbf{h}) \in \mathbb{R}^K, \quad \phi := (\psi, \mathbf{W}_0, \mathbf{W}_1) \quad (5)$$

where $\ell = 0$ for nodes and $\ell = 1$ for edges, *i.e.*, we use different projection for node and edge embeddings before feeding it into the shared MLP network. Optionally, the latent representation \mathbf{h}

[†]Following standard practice [27, 28, 37], we exclude hydrogen atoms from all representations.

can be enriched by concatenating with additional supervision \mathbf{c} , where \mathbf{c} can be given as molecular properties, for use in property-conditioned molecular generation task.

We parameterize the noise schedule for each element (*e.g.*, node) using a weighted combination of polynomial basis functions [56]. For instance, for a i -th node x^i , we use the network output as *coefficients* w^i for the basis, and define the schedule as $\alpha_{t,\phi}^i = \sigma(-\gamma_t^i)$, where $\sigma(\cdot)$ is the sigmoid function and γ_t^i is a noise scheduling network computed via:

$$\gamma_t^i = \hat{\gamma}_t^i \cdot (\gamma_{\max} - \gamma_{\min}) + \gamma_{\min}, \quad \hat{\gamma}_t^i = \frac{\sum_{k=1}^K w_k^i t^k}{\sum_{k=1}^K w_k^i}, \quad (6)$$

where the coefficient w_k^i is k -th element in the output of the noise embedding network $f_\phi(\mathbf{h}^i, 0)$ and the same computation applies analogously to other nodes and edges. Consistent with [31, 56], we fix $\gamma_{\max} = 5$ and $\gamma_{\min} = -13$ for all experiments. Throughout this process, **MELD** naturally introduces element-specific masking rates, mitigating the collapse between distinct molecules that would otherwise persist under unified noise scheduling approaches.

Maintaining gradient flow in discrete sampling. In discrete-space molecular diffusion frameworks [29, 37, 66], the noisy graph at each timestep is obtained by sampling a single graph from a categorical distribution over nodes and edges (Equation 1), as computing the full expectation over $\mathbf{g}_t \sim q(\cdot | \mathbf{g})$ is intractable. However, such discretization introduces a discontinuity in the computational graph when parameterizing the forward process, impeding a gradient flow towards q_ϕ .

To circumvent this issue, we adopt the Straight-Through Gumbel-Softmax (STGS) trick [20], which enables end-to-end training by providing a differentiable surrogate for discrete sampling. Let $\mathbf{z} \in \mathbb{R}^A$ denote the logits over A possible node types, and $\eta > 0$ be the temperature parameter. We first compute a soft approximation of the categorical distribution $\mathbf{p}_{\text{soft}} \in [0, 1]^A$ via the Gumbel-Softmax:

$$\mathbf{p}_{\text{soft},k} = \frac{\exp((z_k + g_k)/\eta)}{\sum_{l=1}^A \exp((z_l + g_l)/\eta)}, \quad (7)$$

where $g_k = -\log(-\log(u_k))$ is a gumbel noise with $u_k \sim \text{Uniform}(0, 1)$ and z_k is the k -th element of the logits \mathbf{z} . A discrete one-hot vector $\mathbf{p}_{\text{hard}} \in \{0, 1\}^A$ is then obtained by taking the index with the highest probability:

$$k^* = \arg \max_k \mathbf{p}_{\text{soft},k}, \quad \mathbf{p}_{\text{hard},k} = \begin{cases} 1 & \text{if } k = k^* \\ 0 & \text{otherwise} \end{cases} \quad (8)$$

To retain gradient flow, we use the straight-through estimator to combine the discrete and continuous components, *i.e.*, set $\mathbf{p} = \mathbf{p}_{\text{hard}} - \text{sg}(\mathbf{p}_{\text{soft}}) + \mathbf{p}_{\text{soft}}$, where $\text{sg}(\cdot)$ denotes the stop-gradient operator. This ensures that the forward pass uses the discretized one-hot vector $\mathbf{p} = \mathbf{p}_{\text{hard}}$, while the backward pass treats \mathbf{p} as the continuous \mathbf{p}_{soft} , allowing gradients to propagate through \mathbf{z} , *i.e.*, $\frac{\partial \mathbf{p}}{\partial \mathbf{z}} = \frac{\partial \mathbf{p}_{\text{soft}}}{\partial \mathbf{z}}$.

4 Experiments

4.1 Experimental setup

We adopt diffusion transformer [49] as a denoising network within a masked diffusion framework. Following prior work [37], we remove the patch-wise embedding from the original implementation to accommodate the graph modality. In property-conditioned generation, we adopt a classifier-free guidance [16] implemented in the original diffusion transformer implementation [37, 49]. We provide additional experimental details in Appendix C.

Datasets. We evaluate **MELD** on two molecular generation settings: unconditional and property-conditioned tasks. For unconditional generation, in line with prior works [27, 28, 33], we use QM9 dataset [52] and ZINC250k [19] datasets. For conditional generation, we employ the Polymer dataset [64] introduced in [37], which conditions homopolymers on three numerical gas permeability constraints (O_2 , N_2 , CO_2) and synthesizability scores.

Table 1: Unconditional generation of 10K molecules on QM9 and ZINC250K datasets. The best and second best performances are represented by **bold** and underline.

Method	QM9						ZINC250K					
	Valid. \uparrow	FCD \downarrow	NSPDK \downarrow	Scaf. \uparrow	Uniq. \uparrow	Novel. \uparrow	Valid. \uparrow	FCD \downarrow	NSPDK \downarrow	Scaf. \uparrow	Uniq. \uparrow	Novel. \uparrow
<i>Flow matching</i>												
MoFlow	91.36	4.47	0.017	0.145	<u>98.65</u>	<u>94.72</u>	63.11	20.93	0.046	0.013	<u>99.99</u>	100.00
GraphAF	74.43	5.63	0.021	0.305	<u>88.64</u>	<u>86.59</u>	68.47	16.02	0.044	0.067	<u>98.64</u>	<u>99.99</u>
GraphDF	93.88	10.93	0.064	0.098	98.58	98.54	90.61	33.55	0.177	0.000	99.63	100.00
<i>Continuous diffusion</i>												
EDP-GNN	47.52	2.68	0.005	0.327	99.25	86.58	82.97	16.74	0.049	0.000	99.79	100.00
GDSS	95.72	2.90	0.003	0.698	98.46	86.27	<u>97.01</u>	14.66	0.019	0.047	99.64	100.00
<i>Discrete diffusion</i>												
DiGress	98.19	0.10	<u>0.0003</u>	0.936	96.67	25.58	94.99	3.48	0.0021	0.416	99.97	<u>99.99</u>
GruM	<u>99.69</u>	<u>0.11</u>	<u>0.0002</u>	0.945	96.90	24.15	98.65	<u>2.26</u>	<u>0.0015</u>	0.530	99.97	<u>99.98</u>
<i>Masked diffusion</i>												
GraphARM	90.25	1.22	0.002	N/A	95.62	70.39	88.23	16.26	0.055	N/A	99.46	100.00
MDM w/ cosine	88.48	3.22	0.005	0.673	92.77	69.31	14.58	27.32	0.047	0.003	100.00	100.00
MDM w/ polynomial	90.37	4.31	0.012	0.694	83.38	64.98	27.78	31.70	0.051	0.004	99.28	100.00
MELD (Ours)	99.72	0.64	<u>0.0003</u>	<u>0.942</u>	95.93	28.14	93.21	2.24	0.0006	<u>0.489</u>	100.00	<u>99.99</u>

Baselines. We consider various recent baselines for conditional and unconditional generation; following experimental setups of prior works [27, 28, 37].

- **Unconditional Generation:** First, we consider three flow-based models as baselines: MoFlow [73], GraphAF [59] and GraphDF [39], three continuous diffusion models: EDP-GNN [47], GDSS [28], and GruM [27], and one discrete-diffusion model: Digress [66]. Additionally, we compare **MELD** against GraphARM [33], a method that employs mask tokens as absorbing states but generates tokens (*i.e.* nodes) autoregressively.
- **Conditional Generation:** We consider four optimization-based frameworks as baselines: GraphGA [23], MARS [70], LSTM-HC [45], and JTVAE-BO [25], two continuous diffusion models: GDSS [28] and MOOD [35], and two discrete diffusion models: DiGress v2 [66] integrated with classifier guidance and GraphDiT [37].

Metrics. Following the evaluation protocol in previous work [27, 28, 37], we evaluate the performance of our framework using the following metrics:

- **Unconditional Generation:** We generate 10,000 samples and evaluate their quality using the following six metrics: (1) *Valid.*, the proportion of chemically valid molecules; (2) *Frechet ChemNet Distance* (FCD) [51], a distributional similarity score between generated and reference molecules based on ChemNet embeddings; (3) *NSPDK* [6], a graph kernel metric that quantifies topological similarity to the reference set; (4) *Scaf.*, a scaffold-level similarity score; (5) *Uniqueness*, the proportion of valid molecules that are structurally distinct within the generated set; and (6) *Novelty*, the fraction of valid molecules not seen in the training data.
- **Conditional Generation:** We generate 10,000 samples and assess their overall quality using the following criteria: (1) *Valid.*, (2) *Cover.*, the heavy atom type coverage; (3) *Divers.*, the diversity among the generated molecules; (4) *Frag.*, a fragment-based similarity metric; and (5) FCD. We also report *Property Alignment*, measured as the mean absolute error (MAE) between target properties and the corresponding oracle-evaluated scores of generated molecules.

To compute property alignment, we follow the setup of prior works [13, 37], employing a random forest model trained on molecular fingerprints as an oracle function.

We collect the values of each baseline reported from prior works [28, 37] for both settings. To evaluate the efficacy of our method in remedying state-clashing within masked-diffusion models, we perform additional ablative studies against fixed-scheduling mechanisms often adopted in masked diffusion models; namely cosine (MDM w/ cosine) and polynomial (MDM w/ polynomial) scheduling.

4.2 Main results

In the following section, we present the results of **MELD** upon benchmark datasets on unconditioned and property-conditioned generation tasks.

Unconditional Generation. We present the results of **MELD** on QM9 [52] and ZINC250K [19] datasets for unconditional generation. As demonstrated in Table 1, **MELD** achieves the best validity

Table 2: Property-conditioned generation of 10K Polymers on three gas permeability properties and synthetic score. The numbers in parentheses in Valid. represent the validity without correction. The best and second best performances are represented by **bold** and underline.

Method	General Quality					Property Alignment				
	Valid. \uparrow	Cover. \uparrow	Divers. \uparrow	Frag. \uparrow	FCD \downarrow	Synth. \downarrow	O ₂ Perm \downarrow	N ₂ Perm \downarrow	CO ₂ Perm \downarrow	MAE \downarrow
<i>Molecule Optimization</i>										
GraphGA	100.00 (N/A)	11/11	88.28	0.927	9.19	1.3307	1.9840	2.2900	1.9489	1.888
MARS	100.00 (N/A)	11/11	83.75	0.928	7.56	1.1658	1.5761	1.8327	1.6074	1.546
LSTM-HC	99.10 (N/A)	10/11	<u>89.18</u>	0.794	18.16	1.4251	1.1003	1.2365	1.0772	1.210
JTVAE-BO	100.00 (N/A)	10/11	73.66	0.729	23.59	1.0714	1.0781	1.2352	1.0978	1.121
<i>Continuous diffusion</i>										
GDSS	92.05 (90.76)	9/11	75.10	0.000	34.26	1.3701	1.0271	1.0820	1.0683	1.137
MOOD	98.66 (92.05)	11/11	83.49	0.023	39.40	1.4019	1.4961	1.7603	1.4748	1.533
<i>Discrete diffusion</i>										
DiGress v2	98.12 (30.57)	11/11	91.05	0.278	21.73	2.7507	1.7130	2.0632	1.6648	2.048
GraphDiT	82.45 (84.37)	11/11	87.12	0.960	<u>6.64</u>	1.2973	<u>0.7440</u>	<u>0.8857</u>	<u>0.7550</u>	<u>0.921</u>
<i>Masked diffusion</i>										
MDM w/ cosine	15.95 (37.16)	11/11	89.91	0.307	26.45	2.1795	1.5035	1.7755	1.4974	1.739
MDM w/ polynomial	18.61 (60.32)	11/11	88.44	0.237	29.32	2.0041	1.6805	1.9846	1.6468	1.829
MELD (Ours)	98.11 (96.50)	11/11	86.04	<u>0.953</u>	6.17	<u>1.1361</u>	0.6084	0.7104	0.6214	0.769

Table 3: Ablation study of **MELD**. The best performances are represented by **bold**.

α_ϕ	Class-wise α_ϕ	Element-wise α_ϕ	Valid. \uparrow	FCD \downarrow	NSPDK \downarrow	Scaf. \uparrow	Uniq. \uparrow	Novel.(%) \uparrow
			27.78	31.70	0.0508	0.004	99.28	100.00
✓	✓		88.58	3.12	0.0009	0.430	100.00	99.97
✓		✓	93.21	2.24	0.0006	0.489	100.00	99.99

in the QM9 dataset, while maintaining competitive performance across another distributional metrics. Notably, our method outperforms GraphARM [33]—the autoregressive masked diffusion baseline—with a 9% increase in validity, a 50% reduction in Fréchet ChemNet Distance (FCD), and an 80% reduction in NSPDK error. On more challenging ZINC250K dataset, which includes larger and more complex molecules, **MELD** sets new state-of-the-art results for both FCD, NSPDK, surpassing GruM [27], the strongest baseline. It also consistently outperforms GraphARM across all metrics. Furthermore, compared to a unified noise schedules, **MELD** improves validity by up to 79%, highlighting its ability to model chemically coherent structures under flexible corruption schemes.

Property-conditioned Generation. Next, we conduct our experiments on conditional generation and report performance of **MELD** on the Polymer [64] dataset, as shown in Table 2. Overall, **MELD** achieves a new state-of-the-art on property alignment, reducing average property MAE by 16% relative to GraphDiT [37]. Apart from GraphDiT, no existing method can satisfy multiple property constraints simultaneously: LSTM-HC achieves strong synthesizability MAE but fails under gas permeability targets. DiGress v2 [66], despite using classifier guidance [8], incurs substantially higher MAE across most conditions. Beyond alignment, **MELD** also improves generative quality, reducing the Fréchet ChemNet Distance (FCD) by 7% over the previous best performance. Consistent with earlier work [16, 38], we observe an inherent trade-off between property alignment and sample diversity. Crucially, **MELD** mitigates the *state-clashing* issue prevalent in masked diffusion: fixed polynomial schedules yield validity below 20%, whereas our learnable, element-wise noise schedule *boosts validity more than 400%* and enhances property alignment by 50% on average, alongside improvements on all other evaluation metrics.

4.3 Ablation study

We evaluate several learnable scheduling strategies on ZINC250K [19] (Table 3) benchmark. The first row represents a standard MDMs with a unified polynomial schedule. In the second row, we implement a class-wise noise scheduling (α_ϕ) method proposed in GenMD4 [60], where each atom and bond type has its own learned corruption rate. The last row corresponds to our **MELD** with element-wise scheduling that learns separate schedules for individual atoms and bonds components, distinguished by parameterized noise representation h .

As depicted in the table, any learnable schedule yields substantial gains in validity and all distributional metrics—an effect we attribute to their ability of reducing state-clashing. Specifically, although

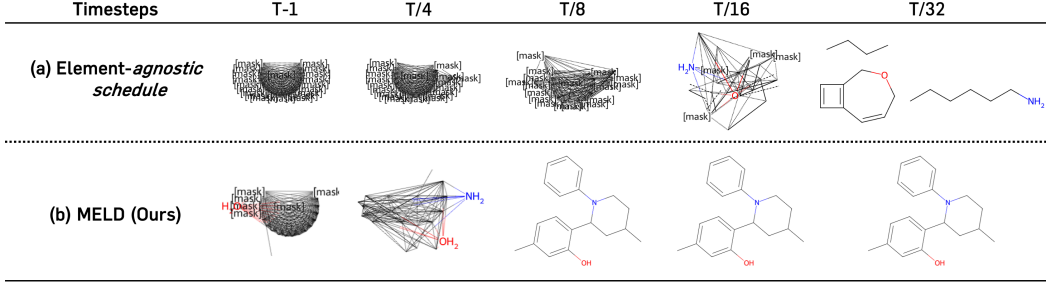


Figure 3: Comparison of (a) fixed polynomial scheduling and (b) **MELD** during reconstruction. With the learnable noise schedule, most reconstruction occurs at earlier timesteps; within the example, Oxygen and Nitrogen nodes are unmasked first, followed by edges and carbon atoms.

employing the parameterized noise scheduling network, class-wise noise scheduling can remain limited in resolving the state-clashing. For example, delaying the corruption of all carbon atoms relative to nitrogen in o-Phenylenediamine may still result in symmetric benzene ring, as illustrated in Figure 1. In contrast, our full per-element corruption technique (**MELD**) delivers an additional 5% gain in validity and further reductions in FCD and NSPDK, confirming the fine-grained control over the forward diffusion trajectory in distinguishing semantically similar elements. This further highlights the efficacy of element-wise learnable noise modeling for chemically sound molecular generation.

4.4 Qualitative analysis

Reverse process of MELD. Figure 3 compares **MELD** against standard, fixed-schedule MDMs. Corrupted nodes and edges are shown as [mask] and dashed lines, respectively. Under the unified noise scheduling, unmasking occurs randomly: at time $t = T/16$ only incoherent fragments emerge, ultimately yielding a broken molecule. In contrast, **MELD** accelerates the reverse process, producing a fully reconstructed molecule by $t = T/8$. Moreover, **MELD** uncovers a clear unmasking hierarchy: the reconstruction of nodes precede that of edges. At step $t = T - 1$, the oxygen atom is revealed first, followed by nitrogen and its bonds, implying that functional groups form before the carbon framework. The similar phenomenon can be found with more examples in Appendix D.2.

Per-element scheduling of MELD. In Figure 4, we visualize the variation in per-step learned noise schedules across nodes and edges during the forward diffusion process. Specifically, we take 200 samples and plot the coefficient of variation (CV) of the conditional probability, defined as $\delta = \sigma/\mu$ where σ and μ denotes the element-wise standard deviation and mean of normalized corruption probability $\frac{\alpha_{t-1,\phi} - \alpha_{t,\phi}}{1 - \alpha_{t,\phi}}$ among sampled elements, respectively. We observe consistently higher variance for edge schedules across all timesteps, suggesting that the model prioritizes differentiating edges more aggressively than nodes during training. As expected, state-clashing problem is inherently intensified in the later steps of the forward process. **MELD**’s effort in discriminating various nodes and edges are focused in the later steps as well, indicated by the peaking variance around $\frac{t}{T} = 0.7$.

5 Conclusion

In this work, we investigated the potential of masked diffusion models (MDMs) for molecular graph generation. We identified a key challenge of applying conventional MDMs in modeling molecules—the *state-clashing* problem, where distinct molecular graphs collapse to indistinguishable intermediate states due to an element-agnostic masking process. To address this, we introduced **MELD**, a masked diffusion framework that learns element-wise corruption trajectories through a parameterized noise scheduling. Extensive experiments demonstrate that **MELD** consistently outperforms baseline MDMs and achieves competitive or superior performance compared to existing diffusion-based methods.

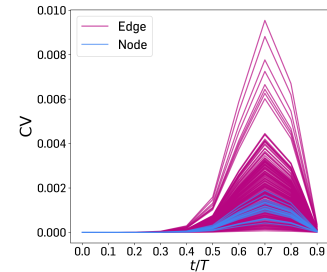


Figure 4: Visualization of the coefficient of variation (CV) across normalized timesteps.

6 Acknowledgments

This work was partly supported by Institute for Information & communications Technology Planning & Evaluation(IITP) grant funded by the Korea government(MSIT) (RS-2019-II190075, Artificial Intelligence Graduate School Support Program(KAIST)), National Research Foundation of Korea(NRF) grant funded by the Ministry of Science and ICT(MSIT) (No. RS-2022-NR072184), GRDC(Global Research Development Center) Cooperative Hub Program through the National Research Foundation of Korea(NRF) grant funded by the Ministry of Science and ICT(MSIT) (No. RS-2024-00436165), the Institute of Information & Communications Technology Planning & Evaluation(IITP) grant funded by the Korea government(MSIT) (RS-2025-02304967, AI Star Fellowship(KAIST)), and Polymerize.

References

- [1] Aye Phyu Phyu Aung, Jay Chaudhary, Ji Wei Yoon, and Senthilnath Jayavelu. Xmol: Explainable multi-property optimization of molecules. *arXiv preprint arXiv:2409.07786*, 2024.
- [2] Jacob Austin, Daniel D. Johnson, Jonathan Ho, Daniel Tarlow, and Rianne van den Berg. Structured denoising diffusion models in discrete state-spaces. In A. Beygelzimer, Y. Dauphin, P. Liang, and J. Wortman Vaughan, editors, *Advances in Neural Information Processing Systems*, 2021.
- [3] Andrew Campbell, Joe Benton, Valentin De Bortoli, Thomas Rainforth, George Deligiannidis, and Arnaud Doucet. A continuous time framework for discrete denoising models. *Advances in Neural Information Processing Systems*, 35:28266–28279, 2022.
- [4] Huiwen Chang, Han Zhang, Jarred Barber, AJ Maschinot, Jose Lezama, Lu Jiang, Ming-Hsuan Yang, Kevin Murphy, William T Freeman, Michael Rubinstein, et al. Muse: Text-to-image generation via masked generative transformers. *arXiv preprint arXiv:2301.00704*, 2023.
- [5] Huiwen Chang, Han Zhang, Lu Jiang, Ce Liu, and William T Freeman. Maskgit: Masked generative image transformer. In *Proceedings of the IEEE/CVF conference on computer vision and pattern recognition*, pages 11315–11325, 2022.
- [6] Fabrizio Costa and Kurt De Grave. Fast neighborhood subgraph pairwise distance kernel. In *Proceedings of the 26th International Conference on Machine Learning*, pages 255–262. Omnipress; Madison, WI, USA, 2010.
- [7] Valentin De Bortoli, James Thornton, Jeremy Heng, and Arnaud Doucet. Diffusion schrödinger bridge with applications to score-based generative modeling. *Advances in Neural Information Processing Systems*, 34:17695–17709, 2021.
- [8] Prafulla Dhariwal and Alexander Nichol. Diffusion models beat gans on image synthesis. *Advances in neural information processing systems*, 34:8780–8794, 2021.
- [9] Yuanqi Du, Arian R Jamasb, Jeff Guo, Tianfan Fu, Charles Harris, Yingheng Wang, Chenru Duan, Pietro Liò, Philippe Schwaller, and Tom L Blundell. Machine learning-aided generative molecular design. *Nature Machine Intelligence*, 6(6):589–604, 2024.
- [10] Vijay Prakash Dwivedi, Anh Tuan Luu, Thomas Laurent, Yoshua Bengio, and Xavier Bresson. Graph neural networks with learnable structural and positional representations. In *International Conference on Learning Representations*, 2022.
- [11] Matthias Fey and Jan E. Lenssen. Fast graph representation learning with PyTorch Geometric. In *ICLR Workshop on Representation Learning on Graphs and Manifolds*, 2019.
- [12] Tianfan Fu, Wenhao Gao, Cao Xiao, Jacob Yasonik, Connor W. Coley, and Jimeng Sun. Differentiable scaffolding tree for molecule optimization. In *International Conference on Learning Representations*, 2022.
- [13] Wenhao Gao, Tianfan Fu, Jimeng Sun, and Connor Coley. Sample efficiency matters: a benchmark for practical molecular optimization. *Advances in neural information processing systems*, 35:21342–21357, 2022.
- [14] Shansan Gong, Mukai Li, Jiangtao Feng, Zhiyong Wu, and Lingpeng Kong. Diffuseq: Sequence to sequence text generation with diffusion models. In *The Eleventh International Conference on Learning Representations*, 2023.
- [15] Jonathan Ho, Ajay Jain, and Pieter Abbeel. Denoising diffusion probabilistic models. *Advances in neural information processing systems*, 33:6840–6851, 2020.
- [16] Jonathan Ho and Tim Salimans. Classifier-free diffusion guidance. In *NeurIPS 2021 Workshop on Deep Generative Models and Downstream Applications*, 2021.
- [17] Emiel Hoogeboom, Didrik Nielsen, Priyank Jaini, Patrick Forré, and Max Welling. Argmax flows and multinomial diffusion: Learning categorical distributions. *Advances in neural*

information processing systems, 34:12454–12465, 2021.

[18] Chenqing Hua, Sitao Luan, Minkai Xu, Zhitao Ying, Jie Fu, Stefano Ermon, and Doina Precup. Mudiff: Unified diffusion for complete molecule generation. In *Proceedings of the Second Learning on Graphs Conference*, volume 231 of *Proceedings of Machine Learning Research*, pages 33:1–33:26. PMLR, 27–30 Nov 2024.

[19] John J Irwin, Teague Sterling, Michael M Mysinger, Erin S Bolstad, and Ryan G Coleman. Zinc: a free tool to discover chemistry for biology. *Journal of chemical information and modeling*, 52(7):1757–1768, 2012.

[20] Eric Jang, Shixiang Gu, and Ben Poole. Categorical reparameterization with gumbel-softmax. In *International Conference on Learning Representations*, 2017.

[21] Yunhui Jang, Dongwoo Kim, and Sungsoo Ahn. Graph generation with k^2 -trees. In *The Twelfth International Conference on Learning Representations*, 2024.

[22] Yunhui Jang, Seul Lee, and Sungsoo Ahn. A simple and scalable representation for graph generation. In *The Twelfth International Conference on Learning Representations*, 2024.

[23] Jan H Jensen. A graph-based genetic algorithm and generative model/monte carlo tree search for the exploration of chemical space. *Chemical science*, 10(12):3567–3572, 2019.

[24] Shuyi Jia, Chao Zhang, and Victor Fung. Llmatdesign: Autonomous materials discovery with large language models. *arXiv preprint arXiv:2406.13163*, 2024.

[25] Wengong Jin, Regina Barzilay, and Tommi Jaakkola. Junction tree variational autoencoder for molecular graph generation. In *Proceedings of the 35th International Conference on Machine Learning*, volume 80 of *Proceedings of Machine Learning Research*, pages 2323–2332. PMLR, 10–15 Jul 2018.

[26] Wengong Jin, Regina Barzilay, and Tommi Jaakkola. Multi-objective molecule generation using interpretable substructures. In *International conference on machine learning*, pages 4849–4859. PMLR, 2020.

[27] Jaehyeong Jo, Dongki Kim, and Sung Ju Hwang. Graph generation with diffusion mixture. In *Proceedings of the 41st International Conference on Machine Learning*, volume 235 of *Proceedings of Machine Learning Research*, pages 22371–22405. PMLR, 21–27 Jul 2024.

[28] Jaehyeong Jo, Seul Lee, and Sung Ju Hwang. Score-based generative modeling of graphs via the system of stochastic differential equations. *arXiv:2202.02514*, 2022.

[29] Thomas J Kerby and Kevin R Moon. Training-free guidance for discrete diffusion models for molecular generation. *arXiv preprint arXiv:2409.07359*, 2024.

[30] Seojin Kim, Jaehyun Nam, Sihyun Yu, Younghoon Shin, and Jinwoo Shin. Data-efficient molecular generation with hierarchical textual inversion. In *International Conference on Machine Learning*, 2024.

[31] Diederik P Kingma, Tim Salimans, Ben Poole, and Jonathan Ho. On density estimation with diffusion models. In A. Beygelzimer, Y. Dauphin, P. Liang, and J. Wortman Vaughan, editors, *Advances in Neural Information Processing Systems*, 2021.

[32] Diederik P Kingma, Max Welling, et al. Auto-encoding variational bayes, 2013.

[33] Lingkai Kong, Jiaming Cui, Haotian Sun, Yuchen Zhuang, B. Aditya Prakash, and Chao Zhang. Autoregressive diffusion model for graph generation. In *Proceedings of the 40th International Conference on Machine Learning*, volume 202 of *Proceedings of Machine Learning Research*, pages 17391–17408. PMLR, 23–29 Jul 2023.

[34] Hannah Lawrence, Vasco Portilheiro, Yan Zhang, and Sékou-Oumar Kaba. Improving equivariant networks with probabilistic symmetry breaking. In *The Thirteenth International Conference on Learning Representations*, 2025.

[35] Seul Lee, Jaehyeong Jo, and Sung Ju Hwang. Exploring chemical space with score-based out-of-distribution generation, 2023.

[36] Xiang Li, John Thickstun, Ishaan Gulrajani, Percy S Liang, and Tatsunori B Hashimoto. Diffusion-lm improves controllable text generation. *Advances in neural information processing systems*, 35:4328–4343, 2022.

[37] Gang Liu, Jiaxin Xu, Tengfei Luo, and Meng Jiang. Graph diffusion transformers for multi-conditional molecular generation. In *The Thirty-eighth Annual Conference on Neural Information Processing Systems*, 2024.

[38] Zhen Liu, Tim Z Xiao, Weiyang Liu, Yoshua Bengio, and Dinghuai Zhang. Efficient diversity-preserving diffusion alignment via gradient-informed gflownets. *arXiv preprint arXiv:2412.07775*, 2024.

[39] Youzhi Luo, Keqiang Yan, and Shuiwang Ji. Graphdf: A discrete flow model for molecular graph generation. In *International conference on machine learning*, pages 7192–7203. PMLR, 2021.

[40] Liheng Ma, Chen Lin, Derek Lim, Adriana Romero-Soriano, Puneet K Dokania, Mark Coates, Philip Torr, and Ser-Nam Lim. Graph inductive biases in transformers without message passing. In *International Conference on Machine Learning*, pages 23321–23337. PMLR, 2023.

[41] Nanye Ma, Mark Goldstein, Michael S Albergo, Nicholas M Boffi, Eric Vanden-Eijnden, and Saining Xie. Sit: Exploring flow and diffusion-based generative models with scalable interpolant transformers. In *European Conference on Computer Vision*, pages 23–40. Springer, 2024.

[42] Amina Mollaysa, Brooks Paige, and Alexandros Kalousis. Goal-directed generation of discrete structures with conditional generative models. *Advances in Neural Information Processing Systems*, 33:21923–21933, 2020.

[43] Matthew Morris, Bernardo Cuenca Grau, and Ian Horrocks. Orbit-equivariant graph neural networks. In *The Twelfth International Conference on Learning Representations*, 2024.

[44] Humza Naveed, Asad Ullah Khan, Shi Qiu, Muhammad Saqib, Saeed Anwar, Muhammad Usman, Naveed Akhtar, Nick Barnes, and Ajmal Mian. A comprehensive overview of large language models. *arXiv preprint arXiv:2307.06435*, 2023.

[45] Daniel Neil, Marwin Segler, Laura Guasch, Mohamed Ahmed, Dean Plumbley, Matthew Sellwood, and Nathan Brown. Exploring deep recurrent models with reinforcement learning for molecule design, 2018.

[46] Alexander Quinn Nichol and Prafulla Dhariwal. Improved denoising diffusion probabilistic models. In *International conference on machine learning*, pages 8162–8171. PMLR, 2021.

[47] Chenhao Niu, Yang Song, Jiaming Song, Shengjia Zhao, Aditya Grover, and Stefano Ermon. Permutation invariant graph generation via score-based generative modeling. In *International conference on artificial intelligence and statistics*, pages 4474–4484. PMLR, 2020.

[48] Adam Paszke, Sam Gross, Francisco Massa, Adam Lerer, James Bradbury, Gregory Chanan, Trevor Killeen, Zeming Lin, Natalia Gimelshein, Luca Antiga, Alban Desmaison, Andreas Kopf, Edward Yang, Zachary DeVito, Martin Raison, Alykhan Tejani, Sasank Chilamkurthy, Benoit Steiner, Lu Fang, Junjie Bai, and Soumith Chintala. Pytorch: An imperative style, high-performance deep learning library. In *Advances in Neural Information Processing Systems* 32, pages 8024–8035. 2019.

[49] William Peebles and Saining Xie. Scalable diffusion models with transformers. In *Proceedings of the IEEE/CVF international conference on computer vision*, pages 4195–4205, 2023.

[50] Stefano Peluchetti. Diffusion bridge mixture transports, schrödinger bridge problems and generative modeling. *Journal of Machine Learning Research*, 24(374):1–51, 2023.

[51] Kristina Preuer, Philipp Renz, Thomas Unterthiner, Sepp Hochreiter, and Gunter Klambauer. Fréchet chemnet distance: a metric for generative models for molecules in drug discovery. *Journal of chemical information and modeling*, 58(9):1736–1741, 2018.

[52] Raghunathan Ramakrishnan, Pavlo O Dral, Matthias Rupp, and O Anatole Von Lilienfeld. Quantum chemistry structures and properties of 134 kilo molecules. *Scientific data*, 1(1):1–7, 2014.

[53] Danilo Rezende and Shakir Mohamed. Variational inference with normalizing flows. In *International conference on machine learning*, pages 1530–1538. PMLR, 2015.

[54] Robin Rombach, Andreas Blattmann, Dominik Lorenz, Patrick Esser, and Björn Ommer. High-resolution image synthesis with latent diffusion models. In *Proceedings of the IEEE/CVF conference on computer vision and pattern recognition*, pages 10684–10695, 2022.

[55] Subham Sahoo, Marianne Arriola, Yair Schiff, Aaron Gokaslan, Edgar Marroquin, Justin Chiu, Alexander Rush, and Volodymyr Kuleshov. Simple and effective masked diffusion language models. *Advances in Neural Information Processing Systems*, 37:130136–130184, 2024.

[56] Subham Sekhar Sahoo, Aaron Gokaslan, Christopher De Sa, and Volodymyr Kuleshov. Diffusion models with learned adaptive noise. In *The Thirty-eighth Annual Conference on Neural Information Processing Systems*, 2024.

[57] Marwin HS Segler, Thierry Kogej, Christian Tyrchan, and Mark P Waller. Generating focused molecule libraries for drug discovery with recurrent neural networks. *ACS central science*, 4(1):120–131, 2018.

[58] Bobak Shahriari, Kevin Swersky, Ziyu Wang, Ryan P Adams, and Nando De Freitas. Taking the human out of the loop: A review of bayesian optimization. *Proceedings of the IEEE*, 104(1):148–175, 2015.

[59] Chence Shi, Minkai Xu, Zhaocheng Zhu, Weinan Zhang, Ming Zhang, and Jian Tang. Graphaf: a flow-based autoregressive model for molecular graph generation. *arXiv preprint arXiv:2001.09382*, 2020.

[60] Jiaxin Shi, Kehang Han, Zhe Wang, Arnaud Doucet, and Michalis Titsias. Simplified and generalized masked diffusion for discrete data. In *The Thirty-eighth Annual Conference on Neural Information Processing Systems*, 2024.

[61] Yuyang Shi, Valentin De Bortoli, Andrew Campbell, and Arnaud Doucet. Diffusion schrödinger bridge matching. *Advances in Neural Information Processing Systems*, 36:62183–62223, 2023.

[62] Martin Simonovsky and Nikos Komodakis. Graphvae: Towards generation of small graphs using variational autoencoders. In *Artificial Neural Networks and Machine Learning–ICANN 2018: 27th International Conference on Artificial Neural Networks, Rhodes, Greece, October 4–7, 2018, Proceedings, Part I* 27, pages 412–422. Springer, 2018.

[63] Yang Song, Jascha Sohl-Dickstein, Diederik P Kingma, Abhishek Kumar, Stefano Ermon, and Ben Poole. Score-based generative modeling through stochastic differential equations. *arXiv preprint arXiv:2011.13456*, 2020.

[64] A Thornton, L Robeson and B Freeman, , and D Uhlmann. Polymer gas separation membrane database. 2012.

[65] Ashish Vaswani, Noam Shazeer, Niki Parmar, Jakob Uszkoreit, Llion Jones, Aidan N Gomez, Łukasz Kaiser, and Illia Polosukhin. Attention is all you need. *Advances in neural information processing systems*, 30, 2017.

[66] Clement Vignac, Igor Krawczuk, Antoine Siraudeau, Bohan Wang, Volkan Cevher, and Pascal Frossard. Digress: Discrete denoising diffusion for graph generation. In *The Eleventh International Conference on Learning Representations*, 2023.

[67] Eric Wang, Samuel Schmidgall, Paul F Jaeger, Fan Zhang, Rory Pilgrim, Yossi Matias, Joelle Barral, David Fleet, and Shekoofeh Azizi. Txgemma: Efficient and agentic llms for therapeutics. *arXiv preprint arXiv:2504.06196*, 2025.

[68] Haorui Wang, Marta Skreta, Cher Tian Ser, Wenhao Gao, Lingkai Kong, Felix Strieth-Kalthoff, Chenru Duan, Yuchen Zhuang, Yue Yu, Yanqiao Zhu, Yuanqi Du, Alan Aspuru-Guzik, Kirill Neklyudov, and Chao Zhang. Efficient evolutionary search over chemical space with large language models. In *The Thirteenth International Conference on Learning Representations*, 2025.

[69] Yuhang Xia, Yongkang Wang, Zhiwei Wang, and Wen Zhang. A comprehensive review of molecular optimization in artificial intelligence-based drug discovery. *Quantitative Biology*, 12(1):15–29, 2024.

[70] Yutong Xie, Chence Shi, Hao Zhou, Yuwei Yang, Weinan Zhang, Yong Yu, and Lei Li. {MARS}: Markov molecular sampling for multi-objective drug discovery. In *International Conference on Learning Representations*, 2021.

[71] S Yang, K Cho, Amil Merchant, Pieter Abbeel, Dale Schuurmans, Igor Mordatch, and Ekin Dogus Cubuk. Scalable diffusion for materials generation. 2024.

[72] Jiaxuan You, Bowen Liu, Zhitao Ying, Vijay Pande, and Jure Leskovec. Graph convolutional policy network for goal-directed molecular graph generation. *Advances in neural information processing systems*, 31, 2018.

[73] Chengxi Zang and Fei Wang. Moflow: an invertible flow model for generating molecular graphs. In *Proceedings of the 26th ACM SIGKDD international conference on knowledge discovery & data mining*, pages 617–626, 2020.

[74] Yiheng Zhu, Jialu Wu, Chaowen Hu, Jiahuan Yan, Tingjun Hou, Jian Wu, et al. Sample-efficient multi-objective molecular optimization with gflownets. *Advances in Neural Information Processing Systems*, 36:79667–79684, 2023.

[75] Zachary Ziegler and Alexander Rush. Latent normalizing flows for discrete sequences. In *International Conference on Machine Learning*, pages 7673–7682. PMLR, 2019.

Supplementary Materials

A More Related Work

Molecule optimization. Optimization-based methods generate molecules by iteratively refining candidates assembled from a predefined vocabulary of fragments, aiming to align with desired property constraints. These approaches typically employ techniques such as genetic algorithms [23], Bayesian optimization [25, 58, 74], and goal-directed generation [42, 72]. Representative examples include [12, 25, 26, 70], which utilize predefined subgraph motifs or scaffolds to ensure chemical validity during the generation process. These methods rely on diverse strategies including Markov sampling to sparse Gaussian processes and optimize molecules based on property-specific scoring functions. Goal-directed generation [42, 72], in particular, often adopts reinforcement learning, where a generation policy is updated to maximize a property-driven reward function. Despite their strengths, existing optimization-based approaches remain limited in conditional generation settings. Specifically, they require a full re-optimization for each new property configuration when tasked with generating molecules that precisely match target properties, rather than simply increasing or decreasing property values. This results in a high training complexity and limits their scalability [1, 69].

Learnable noise scheduling. Several works have explored learnable corruption process to optimize the forward trajectories in images and text. In continuous-space diffusion models, [31] introduces a learnable scalar noise schedule as a function of time, enabling variance reduction in evidence lower bound (ELBO) estimation. Extending this, [56] proposes a multivariate, data-dependent noise schedule, showing that a non-scalar, adaptive diffusion process can further tighten the ELBO by aligning the forward process more closely with the true posterior. In discrete masked diffusion, [60] generalizes the corruption process to allow class-dependent masking rates across tokens, prioritizing semantically important tokens during generation. Additionally, Schrödinger bridges-based approaches [7, 50, 61] formulate generative modeling as learning an expressive, path-wise forward process by solving entropy-regularized optimal transport problems over path spaces.

It is noteworthy that the design philosophy of **MELD** is built upon the state-clashing problem, a critical issue that has not been addressed in these work nor in the molecular diffusion literature [27, 28, 35, 37, 66]. While employing the learnable forward process paradigm, our work departs from existing methods by introducing graph element-wise parameterization of the forward diffusion, specifically to avoid trajectory collisions between semantically distinct molecules. Moreover, we explicitly target and resolves the intermediate state degeneracy unique to discrete molecular graphs, while Schrödinger bridge approaches does not directly address discrete structural collapse.

B Limitations and Broader Impact

While our element-wise noise scheduling significantly mitigates the state-clashing issue, it may not fully address the inherent multimodality when a large portion of molecules are masked at later diffusion steps. This is especially pronounced at later diffusion steps, where a majority of the graph elements are masked, making it challenging to distinguish them.

From a broader perspective, **MELD** has a potential to accelerate molecular discovery and reduce the need for costly and time-intensive wet-lab experiments, thereby contributing to advancements in drug design and material science. However, as with any generative technology, there exists the risk of misuse, including the malicious design of toxic or harmful compounds. We advocate for the responsible deployment of such models for the safe integration into real-world workflows.

C Implementation Details

Table 4: Dataset statistics.

Dataset	#(Graphs)	#(Nodes)	#(Node types)	#(Edge types)
QM9	133,985	$ \mathcal{V} \leq 9$	4	3
ZINC250K	249,555	$ \mathcal{V} \leq 38$	9	3
Polymers	553	$ \mathcal{V} \leq 50$	11	3

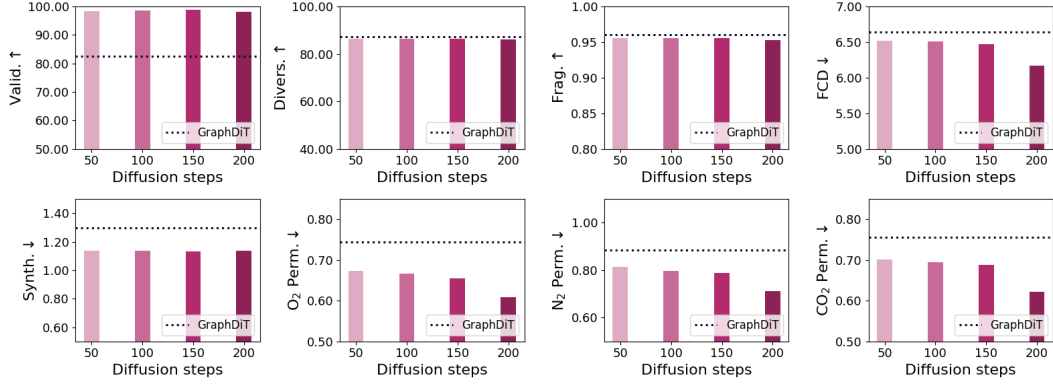


Figure 5: Performance of **MELD** under varying diffusion steps. The dotted line indicates the performance of the strongest baseline, GraphDiT [37], evaluated at a fixed diffusion step of 500.

We follow the evaluation protocols and dataset splits adopted in prior works: for unconditional generation, we adopt the setup from [27], and for property-conditioned tasks, we follow the procedure outlined in [37]. We provide the detailed statistics of each dataset in Table 4. During training for unconditional generation, we apply an exponential moving average (EMA) to the model parameters, consistent with the training framework in [27]. For conditional generation, we utilize the implementation strategies proposed in [37, 49], including condition vector encoders and adaptive layer normalization (AdaLN). All models are implemented in PyTorch [48] with PyTorch Geometric [11]. Experiments were conducted on machines equipped with NVIDIA RTX 4090 and A5000 GPUs (24 GB) and AMD EPYC 7543 32-Core CPUs (64 cores total). Across all experiments, we use a transformer-based denoising model [49] with 6 layers, a hidden dimension of 1152, and 16 attention heads. The noise scheduling network is parameterized as a two-layered MLP with SiLU activation with hidden dimension set as 64. We train all models using the AdamW optimizer with batch sizes between [512, 1024], no weight decay, and a fixed random seed of 0.

D Further Experiments and Analysis

D.1 Robustness across different diffusion steps

We evaluate the performance of **MELD** on the Polymer dataset under varying diffusion steps, setting the total timestep $T \in \{50, 100, 150, 200\}$. Note that during this experiment, we fix the **MELD**-incorporated MDM to be trained upon a fixed diffusion step of 200, and only vary the number of steps taken during inference. We compare the performance of **MELD** against that of the strongest baseline, GraphDiT [37], which is originally evaluated at diffusion step size of 500. As depicted in Figure 5, **MELD** overall exhibits robust performance across a range of metrics. Interestingly, for validity, diversity and fragment similarity and synthesizability, we see consistent performance across diffusion steps. However, for Fréchet ChemNet Distance (FCD), O₂, N₂, and CO₂ permeability, we see monotonic gains in performance as we increase the diffusion step size.

D.2 More examples of reverse process in MELD

We present additional visualizations of the reverse diffusion trajectories under **MELD** alongside those obtained via a fixed polynomial (element-agnostic) schedule in Figure 6. Consistent with our earlier analysis, **MELD** exhibits a clear denoising hierarchy: node attributes are restored prior to edge attributes. By contrast, the element-agnostic schedule—lacking any element-specific ordering—produces severely distorted molecular graphs even at late timesteps. For example, at timestep $T/16$, when the majority of graph tokens have been recovered, the fixed schedule still fails to reveal coherent substructures, resulting in chemically invalid molecules.

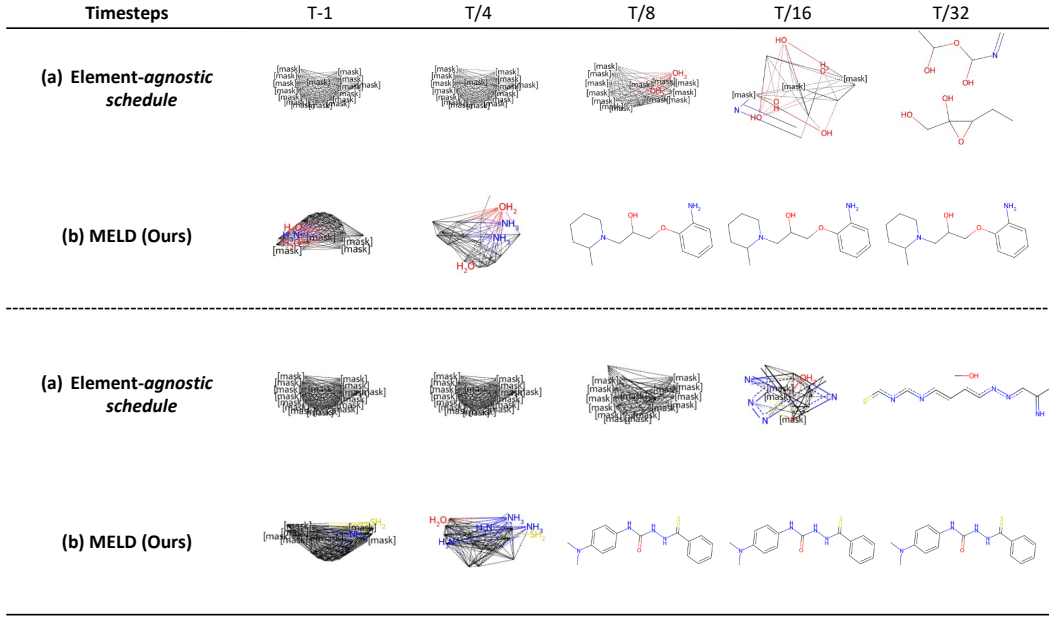


Figure 6: Comparison of (a) fixed polynomial scheduling and (b) **MELD** during reconstruction on the ZINC250K dataset. With the learnable noise schedule, most reconstruction occurs at earlier timesteps.

D.3 Molecule visualization

In this section, we provide 2D visualization of molecules generated by **MELD**. As illustrated, **MELD** generates chemically realistic molecules even for polymers dataset with larger number of atoms (*i.e.*, $|\mathcal{V}| \leq 50$), confirming its robustness under various graph sizes.

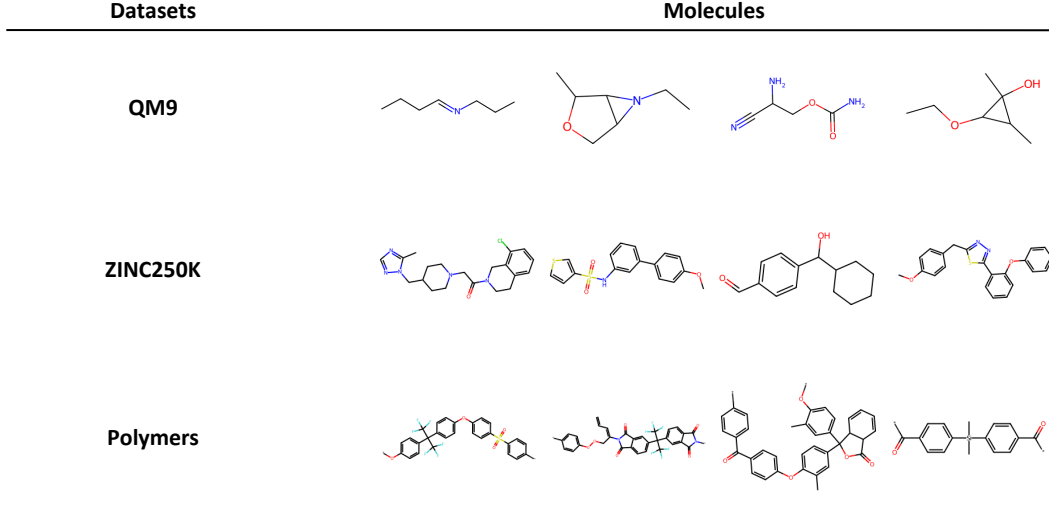


Figure 7: Visualization of molecules generated by **MELD**.